The present horizontal kinematic pattern in the Eastern Europe Region inferred from the GNSS observation

Cenni[(1)] N., Caporali[(1,2)] A., Zurutuza[(1,2)] J., Bertocco[(2)] M.
(1) Department of Geosciences – University of Padova
(2) Centro di Ateneo di Studi e Attività Spaziali " Giuseppe Colombo" – CISAS – University of Padova

CEGRN Network

The Central European GPS Geodynamic Reference Network Consortium (CEGRN) is a GNSS Permanent Network that covers a large area in Central-Eastern Europe (Figure 1). Thanks to the contributions of several Agencies, that provide either RINEX or SINEX files, that latest solution consists of more than 1100 sites, including EPN stations. These stations are regularly computed using the EUREF CB guidelines and the results are used for a number of different applications, such as geophysical research or professional use. The first CEGRN campaign took place in 1995.
After the 199 and 1997 surveys, the campaigns are observed in mid-June each 2 years and were recomputed using repro2 products (IGb08 compliant). However, because most of the former stations were epoch-sites and the fact that many of the SINEX files that were provided were not repro2-based, in this work we will show the results available from GPS week 1632 – 1953 (2011-04-17 to 2017-01-29) in order to avoid problems introduced by the different datum/models used in non-repro2 solutions and the former epoch sites.
The Figure 2 and 3 show the horizontal and vertical velocity patterns obtained by the multi-year adjustment of the files available from 2011-2017. The solution is aligned to the C1934 EPN release (A Class stations) by imposing the minimum constraints condition (solving only from translations) and the computed velocities span at least over 2 years of observation; A Class velocities are heavily constrained to their published values (10^{-7}). The quality of the result is checked by means of a Helmert transformation, where the computed A Class stations are compared with their nominal value. A summary of the statistics of these residuals is shown in Table1. The velocities values are obtained by a least square weighted approach using the following weekly solutions: 1641 (2011/06/19), 1745 (2013/06/16); 1849 (2015/06/14) and 1953 (2017/06/11). For more details see the oral presentation of Zurutuza J. et al. during the meeting.

	RMS	Mean	Min	Max
North	1.1	0.0	-4.8	2.6
East	1.0	0.0	-3.2	9.8
Vertical	2.3	0.0	9.8	7.8

Table 1. Statistics of the residual values obtained comparing the velocities estimated in the CEGRN analysis of the A Class sites considered in the network (red dots in Figure 1) and the nominal values reported in the C1934 EPN release. The first column contains the Root Mean Square (RMS) of the difference distribution for each component of the velocity, in the second there is the mean and in the last two the Minimum (Min) and Maximum (Max) values of the differences. All values reported are in mm/yr.

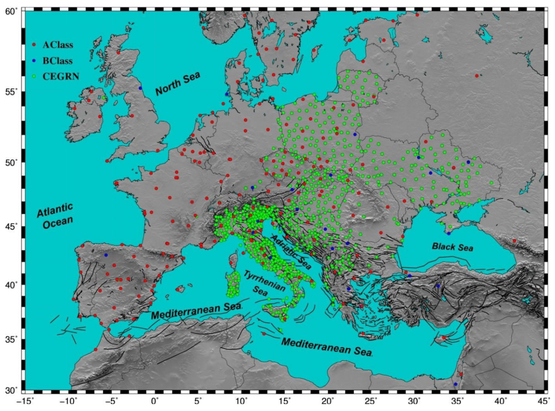

Figure 1. The CEGRN GNSS Permanent Network. Red, blue and green dots represent A and B Class Euref sites and CEGRN stations respectively. The database of seismogenic sources of the Euro-Mediterranean area (SHARE project, Basili et al. 2011) is also shown, the black lines indicate the fault top trace.

Figure 2. Residual horizontal velocity field respect to the Eurasian plate. Red, blue and green dots represent A and B Class Euref sites and CEGRN stations respectively. The database of seismogenic sources of the Euro-Mediterranean area (SHARE project, Basili et al. 2011) is also shown, the black lines indicate the fault top trace. The circles show the position of the GNSS permanent stations and the colour shows the module of the horizontal velocity in mm/yr following the chromatic scale on the figure.

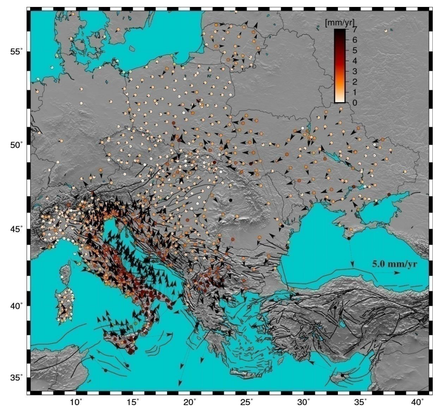

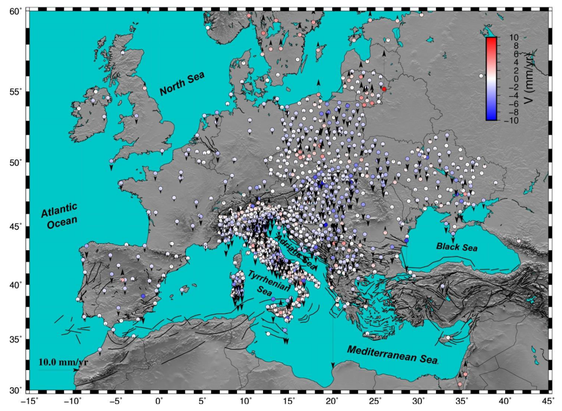

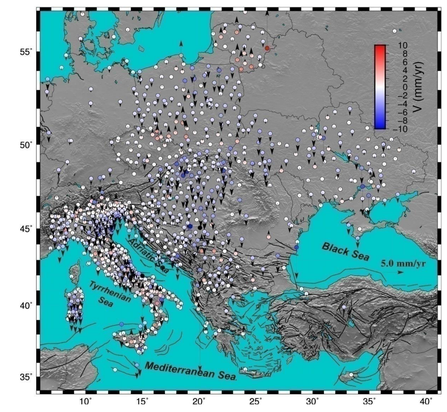

Figure 3. Vertical velocity field of the CEGRN network in the IGb08 Reference frame. The colours of the circles show the velocity amplitudes in mm/yr following the chromatic scale on the figure.

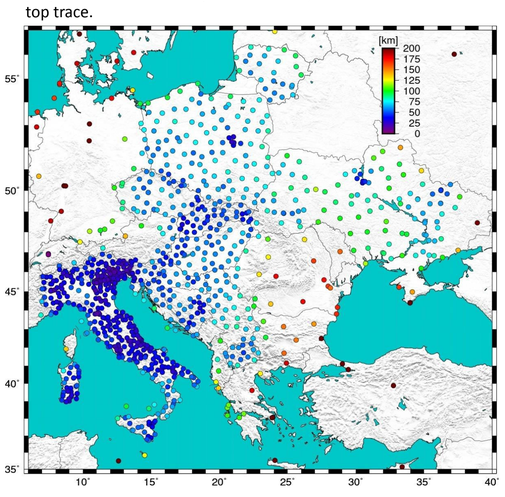

Figure 4. Interdistance between the i-th stations and the 'fourth nearest sites'. For each GNSS sites we have estimate the distance between the i-th site and the other stations belonging to the network. Successively this distance array has been shorted in increasing order, therefore in this array in the fourth position there is the minimum distance for which the geometric criteria described in the text is satisfied. The colours of the circles show the distance between the i-th sites and the stations collocated at the fourth position in the 'distance' array ('fourth nearest sites') following the chromatic scale on the figure.

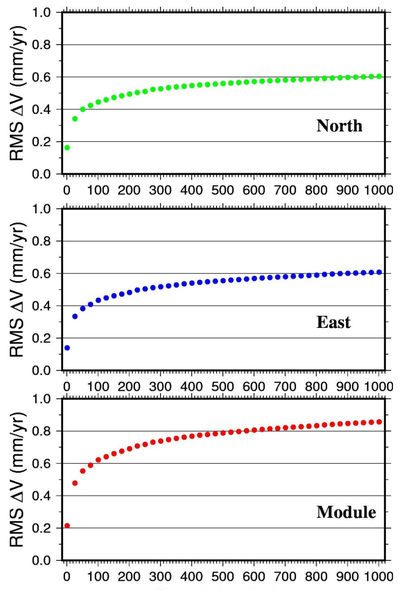

Figure 5. Statistics of the differences between the GNSS observed velocities and the values estimated with collocation approach by different smoothing factors. Root mean square (RMS) of the differences between the values components north and east of the velocity and module.

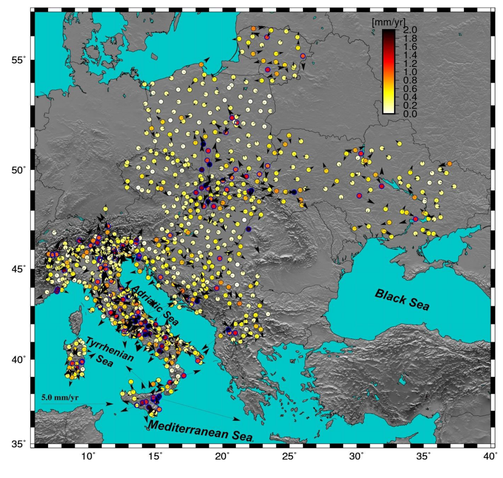

Figure 6. Velocity difference between the values estimated analyzing the GNSS observation and the ones obtained by the collocation approach with a smoothing factor equal 301. The colours of the circles show the module of difference in mm/yr following the chromatic scale on the figure. The velocity field outliers detected with the LSC approach are indicated as a blue circle.

Last Square Collocation Approach

The movements observed by the GNSS technique can be considered as the combination of the displacements due to different phenomena as, for example: global, regional and local tectonic processes, climatologic and meteorological phenomena and human activities. The principal aim of this work is to highlight the movements due to the main geodynamic processes involved in the Central and Eastern Europe. Therefore the local movements due to other sources should be remove from the velocity field or mitigate. Usually these displacements are observed by a few number of stations, often only one if the interdistance between the stations is about of few tens of kilometres. In order to avoid that the velocity field and deformation pattern could be influenced by these spurious values, it is necessary to develop a filter able to detect these anomalies. A method can be developed starting from the least squares collocation (LSC) algorithm proposed to Caporali et al. (2003, 2009, 2018), where the velocity at a point P can be estimated as a weighted average of the velocities observed in N GNSS sites closely at this point:

$$v_p = \sum_{k=1}^{N} a_{pk} v_k + \epsilon_p \qquad (1)$$

where N is the number of GNSS stations and e_p the model error. The coefficients a_{pk} can be estimated minimizing the error variance as suggest in the Caporali et al. 2018, in order to solve the equation can be introduced the correlation function C, and the coefficients a_{pK} can estimated solving this equation:

$$a_{pk} = \sum_{i=1}^{N} \sum_{k=1}^{N} C_{p_i} C_{ik}^{-1} \qquad (2)$$

The correlation function C depends on the square of the ratio of the distance d between pairs of station and a correlation distance d_0, in particular:

$$C_{p_i} = \frac{1}{1 + \left(\frac{d_{p_i}}{d_0}\right)^2} \qquad (3)$$

where;

$$d_{p_i} = \sqrt{(E_p - E_i)^2 + (N_p - N_i)^2} \qquad (4)$$

E and N are the cartographic East and North components of the site position. The horizontal velocity (East and North components) at a point P can be estimated as:

$$\begin{bmatrix} v_{eP} \\ v_{nP} \end{bmatrix} = \sum_{i=1}^{N} C_{p_i} C_{ik}^{-1} \begin{bmatrix} v_{ek} \\ v_{nk} \end{bmatrix} \qquad (5)$$

The velocity at a point P is a function of the distances d between the sites considered in the analysis and the correlation distance d_0. In order to take into account the uncertainties associated to the velocities estimated it can be introduced the covariance matrix of the measuring errors (Moritz 1978):

$$W_{ij} = \frac{\sigma_i^2}{\sum_{k=1}^{N} \sigma_k^2} \delta_{ij} \qquad (6)$$

where σ_i is the uncertainties associated at the East and North velocity component. The weighted matrix can be introduced in the collocation algorithm modifying the correlation function:

$$C_{ik} = C_{ik} + W_{ik} \qquad (7)$$

The definition of correlation function in equation (7) takes into account the uncertainties associated to the velocity values and the equation 5 can be rewritten as:

$$\begin{bmatrix} v_{eP} \\ v_{nP} \end{bmatrix} = \sum_{i=1}^{N} C_{p_i} \sum_{k=1}^{N} (C_{ik} + W_{ik})^{-1} \begin{bmatrix} v_{ek} \\ v_{nk} \end{bmatrix} \qquad (8)$$

The strain rate at a point P can be estimated by the horizontal gradient in the East and North direction of the velocity v_p :

$$\begin{cases} \frac{\partial \vec{v}_p}{\partial E_p} = \sum_{i=1}^{N} \frac{\partial C_{p_i}}{\partial E_p} C_{ik}^{-1} \vec{v}_k \\ \frac{\partial \vec{v}_p}{\partial N_p} = \sum_{i=1}^{N} \frac{\partial C_{p_i}}{\partial N_p} C_{ik}^{-1} \vec{v}_k \end{cases} \qquad (9)$$

with

$$\frac{\partial C_{p_i}}{\partial E_p} = -2(C_{p_i})^2 \frac{(E_p - E_i)}{d_0^2} \qquad \frac{\partial C_{p_i}}{\partial N_p} = -2(C_{p_i})^2 \frac{(N_p - N_i)}{d_0^2} \qquad (10)$$

The strain rate matrix at a point P is:

$$\begin{bmatrix} \varepsilon_{ee} & \varepsilon_{en} \\ \varepsilon_{ne} & \varepsilon_{nn} \end{bmatrix} = \sum_{i=1}^{N} \sum_{k=1}^{N} \begin{bmatrix} \frac{\partial C_{p_i}}{\partial E_p} & \frac{\partial C_{p_i}}{\partial N_p} \\ \frac{\partial C_{p_i}}{\partial E_p} & \frac{\partial C_{p_i}}{\partial N_p} \end{bmatrix} (C_{ik} + W_{ik})^{-1} \begin{bmatrix} v_{ek} \\ v_{nk} \end{bmatrix} \qquad (11)$$

The velocity and strain rate at a point P can be estimated by equations (8) and (11). It can be noted as this method depends on an 'user' parameter: the correlation distance. This value can be imposed by the user or searched within a range by a criterion chosen to the user, for example the correlation distance associated to the maximum values of the shear strain rate or the maximum value of the strain rate trace. Also, in order to improve the reliability of the velocity and strain rate values estimated, we have introduced an additional geometric criteria: the velocity component are taken as acceptable only when at least four GNSS sites are located at a distance lower than d0 from the point considered. Among the different possible options about the correlation distance, in this work we have chosen to estimate this value as that corresponding at the maximum value of the shear strain rate. The correlation distance range imposed is equal for all points considered in the procedure. Some indications about the correlation distance range can provide from the interdistance between the sites belonging the network considered. For each sites we have estimate the distance with the other stations and shorted in increasing order, therefore in this array in the fourth position there is the minimum distance for which the geometric criteria is satisfied. The Figure 4 shows the distance between the i-th sites and the stations collocated at the fourth position of the 'distance' array described before. It can be noted as the Italian GNSS sites area characterized by a distance of about 30-50 Km; instead of this value is significantly greater than 70 Km for the sites located in the Central an Easter European area. In order to take into account this characteristic we chose to adopted, in the collocation least squares algorithm a range for the correlation distance d0 between 70 Km 150 Km. The regional strain rate pattern in the Central and Eastern Europe area could be estimated by equation (11) using the dense velocity field shows in Figure 2. But it could be strongly influenced from the spurious velocity values. These rates, probably due to local geological/geophysical and antropogenetic phenomena, could mask the real kinematic patter due to the regional geodynamic processes. Therefore, before to estimate the deformation pattern it is necessary to detect these outliers in the velocity field and mitigate their effects in the strain rate estimation procedure. A possible method in order to detect the velocity outliers can be developed modifying the previous least square collocation approach, introducing an additional smoothing parameter in the definition of weighted matrix:

$$W_{ij} = \left(\frac{\sigma_i^2}{\sum_{k=1}^{N} \sigma_k^2} \delta_{ij} \right) * sf \qquad (12)$$

where the sf is the smoothing factor, it is an adimensional parameter with values greater than 1. This parameter provides the possibility to estimate the velocity at a point P smoothing the influence of the nearest GNSS stations and emphasizing the influence of the sites located at a relatively medium distance. If the point P is the position of a GNSS station, by this parameter it is possible to estimate the velocity due the nearest GNSS sites, smoothing the influence of the velocity observed in that point. If the difference between the estimated and the GNSS observed velocity value is significative, for example, greater than 1 mm/yr, the site can be considered as an outlier and in the successively strain rate estimation procedure considered with a weight lower than the other sites. In order to evaluated the best value of the smoothing factor, we have estimated by the collocation approach the horizontal velocity field in the position of the GNSS sites using different values of sf between 1 to 1001 with a step of 25. The Figure 5 shows the trend of the root mean square (RMS) of differences between the observed (GNSS) and estimated value of the north and east component of the velocity, respect to the smoothing factor parameter. The RMS trend of the difference velocity modulus is also shown in Figure 5. It can be noted has the RMS value is almost constant (i.e. the increasing is lower than 5%) after a sf equal to 301. This means that the smoothing effects of the parameter sf do not change for values greater than 301, and therefore this value has been adopted in the outliers search. The Figure 6 shows the differences between the GNSS velocities and the values estimated by the least square collocation approach with a smoothing factor equal to 301. The velocity values are not estimated on 222 sites, where the geometrical criteria are not satisfied. We have defined as outlier of velocity field the sites where the difference between the horizontal GNSS velocity and the LSC estimated values is greater than 0.9 mm/yr. The permanent stations in Figure 6 with circle blue line are the 120 sites identifies as outlier, they are about 13% of the 892 sites considered in the LSC analysis. In order to mitigate the influence of the outliers in the strain rate estimation procedure we have introduced an additional weighted matrix W^0 in the equation (7):

$$C_{ik} = C_{ik} + (W_{ik} * W_{ik}^0) \qquad (13)$$

The additional weighted matrix W^0 is a diagonal matrix with the diagonal terms equal to 10 in correspondence of the stations characterize by an outlier velocity values, and 1 otherwise.

Present kinematic pattern in the Central and Eastern European area

We have investigated the present kinematic and deformation pattern in the Central and Eastern European area analyzing by a least square collocation approach the GNSS horizontal velocity field showed in Figure 2. In particular, we focus on the regional geological/geophysical processes with a wavelength greater than about 100 Km, due to the major tectonic features showed in the Figure 7. The horizontal velocity and strain rate tensor on the nodes of a regular grid of 0.25° x 0.25° have been estimated by equation 8 and 11 with a smoothing factor of 301. The sites detected as outlier of velocity field (Figure 6) are also considered with different weights (equation 13). The horizontal velocity and the strain rate matrix have been computed only in the nodes where the geometrical criterion, introduced in the LSC paragraph, has been satisfied. The correlation distance d0 corresponding at the maximum value of the shear strain rate has been adopted as the criterion in order to estimate the horizontal velocity field and the shear strain rate pattern showed in Figure 8 and 9 respectively. In order to avoid nodes with a number of shear strain rate estimation significatively different, the nodes where these values have been estimated using a number of correlation distance lower than 4 are not included in the successively analysis and in the figure 8 and 9. The shear strain rate contouring map showed in Figure 8 should be considered reliable only in the areas where the values are effectively estimated. The position of colour circles in Figure 8 and 10 indicates the zones where the algorithm computes the velocity and strain rate and therefore where the contouring map is reliable. The Figure 10 shows the correlation distance d_0 distribution corresponding to the maximum shear strain rate. It can be noted as a large number of grid points is characterized by d_0 values lower than the upper limit of the search range (150 Km). When the maximum shear strain has been estimated by the largest values of the correlation distance range this mean that the tectonic process located in the area are not well defined. Therefore, the results showed in figure 10 suggests that in large sectors of the study area the velocity estimated could be considered as representative of the tectonic processes located in the Central- Eastern Europe.
The velocity values (Fig. 8) estimated in several regions of the study area, for example in the Pannonia basin, Poland, Lithuania and Ukraine state (Fig. 7) are at the limit of the resolving power of the GNSS technique, lower than about 1 mm/yr. Nevertheless, the kinematic and deformation patterns show some interesting features. In particular, it can be noted as the velocities of the nodes located on the Northern sector of the East Lithuanian domain (ELd Fig.7, Skridlaite et al. 2003) are characterized by a N-E direction significantly different to ones located on the West Granulite Lithuanian domain (WGLd Fig. 7, Skridlaite et al. 2003) where the velocities are about null and in South part of ELd where the rate are characterized by a SW direction. The horizontal velocity field estimated in the Ukraine area points out the presence of fairly coherent regimes in the various tectonic units (Fig. 7 and 8); even if the differences observed are lower than the resolving power of the GNSS technique and the velocity field in each zone shows a non coherent pattern. The Dnieper-Donets rift area (DDR) is characterized by a scarce mobility (velocity module lower than 1 mm/yr), while the nodes located on the Ukrainian Shield and Volyn-Podilla plate (US and VPP Fig. 7 and 8) are characterized by a more faster mobility with velocities greater than 1 mm/yr. In this context the deformation pattern of the region should be characterized by a moderate extensional regime, the relative maximum shear strain rate values observed in the area (Fig. 9) could be due to a local movements that introduce a short wavelength signals in the deformation pattern. Figure 8 shows that the Dinaridies area (Internal and External sectors, Fig. 7) moves significantly faster (3-6 mm/yr) respect to the other regions with a direction about N-E respect an Eurasian fixed reference frame. In particular, the nodes located on the external part of the belt (Ext. Din. Fig. 7) are characterized by modules greater than ones located on the Internal part. This results it is coherent with the others geological and geophysical evidences that indicates the Dinaridies as a thrust and fold belt formed during the collision between the Adria and Eurasian plate (i.e. Kastelic and Carafa 2012 and reference therein). The greatest values of the shear strain rate showed in Figure 9 can be detected in the North and South boundaries of the Dinaridies domain in correspondence of the Albania fault system (AF, Fig. 7) and Zagreb-Zemplen lineament (ZZL, Fig. 7). These results are in agreement with the hypothesis that the AF could represent a lateral decoupling fault system between the southern Dinaridies sector and Hellenides (Mantovani et al. 2000); and the shear behavior of the ZZL lineament suggested to different authors (e.g. Tomljenovic et al. 2008; Tomljenovic and Csontos, 2001). The tectonic complexity of these areas induce obviously a more detailed studies in order to improve and confirm the agreement between geodetic and geological/geophysical observations.

Figure 7. The geodynamic settings in the Central- Eastern European region. The thick black lines indicate the top trace of the faults from the Euro-Mediterranean database of seismogenic sources (SHARE project, Basili et al. 2011). The thin black lines show the principal tectonic structures in the Pannonian basin (modified from Bada et al. 2001 and Hetenyi et al. 2006). AF = Albania Fault system. AlCaPa = Alpine–Carpathian–Pannonian terrain; BM = Bohemian Massif; BF = Balaton Fault (Bada et al. 2001, Hetenyi et al. 2006); BSD = Black sea depression (Bezvynniy et al. 2006); DDR = Dnieper-Donets rift (Bezvynniy et al. 2006); E.A. = Eastern Alps; E. Carp. = East Carphatians; KS= Kovel salient (Bezvynniy et al. 2006); MHF = Mid Hungarian Fault (Bada et al. 2001, Hetenyi et al. 2006); MMZ = Mur-MURZ-Zilina line (Bada et al. 2001, Hetenyi et al. 2006); N.A.F. = North Anatolian Fault; PB = Pannonian –Basin; RM = Rhodope Massif; S. Carp. = South Carphatians; TD= Tisza-Dacia unit; US = Ukrainian Shield (Bezvynniy et al. 2006); VPP= Volyn-Podilla plate (Bezvynniy et al. 2006); W. Carp. = West Carphatians; WLGd= West Lithuanian Granulite domain (Skridlaite et al. 2003); ZZL = Zagreb-Zemplen lineament.

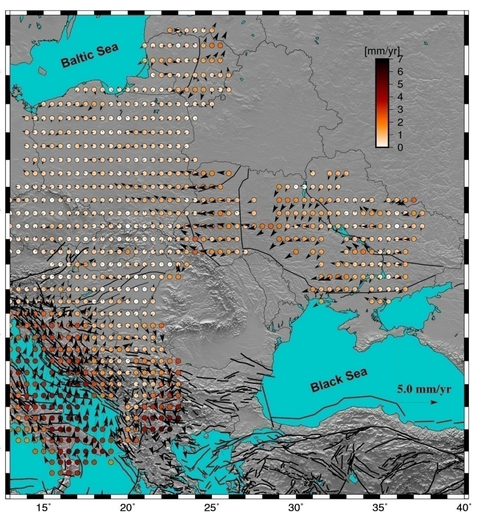

Figure 8. Interpolated horizontal velocity field. The colours of the circles show the velocity module in mm/yr following the chromatic scale on the figure. In order to highlight the principal characteristics of the velocity pattern, in the figure are showed only the vectors corresponding at the nodes of a regular grid 0.5° x 0.5°. The thick and thin black lines show the principal tectonic structures in the study area as described in Figure 7.

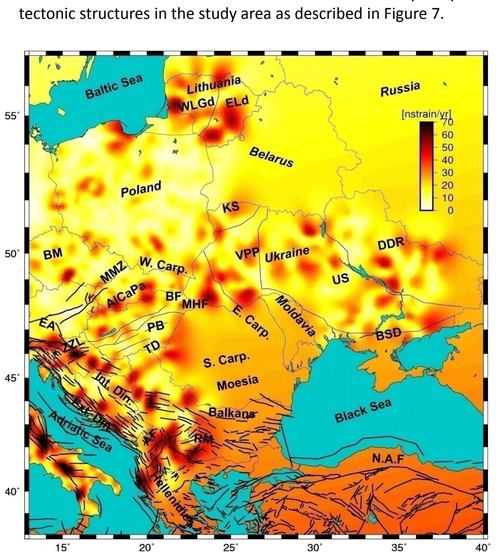

Figure 9. Maximum shear strain rate pattern estimated by the LSC approach on the nodes of a regular grid of 0.25° x 0.25°, with a smoothing factor equal 301. In each grid node, where the geometrical criterion has been satisfied, the strain rate has been estimated using different values of correlation distance d_0 since 70 Km to 150 Km, with a step of 10 Km. For each correlation distance has been estimated the shear strain rate values and searched the maximum value showed in figure. The correlation distance corresponding at the maximum values are showed in Figure 10. The contouring of the shear strain rate should be considered reliable only in the areas where these values are effectively estimated, i.e. where the the geometrical criterion has been satisfied and it has possible estimate at least 5 strain rate values with different correlation distance. The position of the circles in Figure 8 and 10 indicate the areas where these condition are satisfied. The black lines and acronym show the principal tectonic structures in the study area as described in Figure 7.

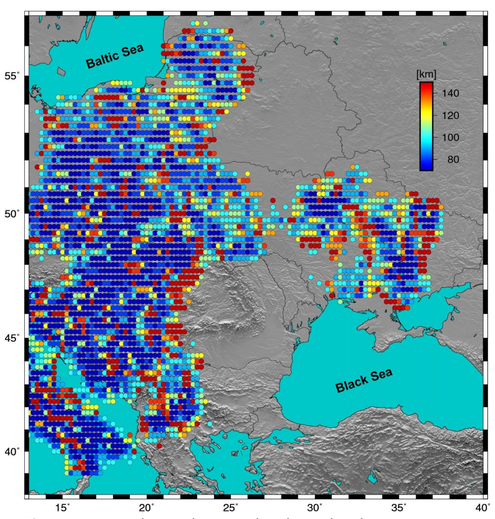

Figure 10. Correlation distance d0 where the shear strain rate achieves the maximum value (Figure 10), see the text or the Figure 9 Caption for more details. The colour of the circles correspond at the distance in Km following the chromatic scale on the figure.